

Focal-point approach with pair-specific cusp correction for coupled-cluster theory

Andreas Irmler,* Alejandro Gallo, and Andreas Grüneis

*Institute for Theoretical Physics, TU Wien,
Wiedner Hauptstraße 8–10/136, 1040 Vienna, Austria*

(Dated: March 12, 2021)

We present a basis set correction scheme for the coupled-cluster singles and doubles (CCSD) method. The scheme is based on employing frozen natural orbitals (FNOs) and diagrammatically decomposed contributions to the electronic correlation energy that dominate the basis set incompleteness error (BSIE). As recently discussed in [Phys. Rev. Lett. 123, 156401 (2019)], the BSIE of the CCSD correlation energy is dominated by the second-order Møller-Plesset (MP2) perturbation energy and the particle-particle ladder term. Here, we derive a simple approximation to the BSIE of the particle-particle ladder term that effectively corresponds to a rescaled pair-specific MP2 BSIE, where the scaling factor depends on the spatially averaged correlation hole depth of the coupled-cluster and first-order pair wavefunctions. The evaluation of the derived expressions is simple to implement in any existing code. We demonstrate the effectiveness of the method for the uniform electron gas. Furthermore, we apply the method to coupled-cluster theory calculations of atoms and molecules using FNOs. Employing the proposed correction and an increasing number of FNOs per occupied orbital, we demonstrate for a test set that rapidly convergent closed and open-shell reaction energies, atomization energies, electron affinities, and ionization potentials can be obtained. Moreover, we show that a similarly excellent trade-off between required virtual orbital basis set size and remaining BSIEs can be achieved for the perturbative triples contribution to the CCSD(T) energy employing FNOs and the (T*) approximation.

I. INTRODUCTION

Traditional quantum chemical theories approximate the many-electron wavefunction by a linear combination of Slater determinants constructed from one-electron orbitals. Unfortunately, this expansion causes a frustratingly slow convergence of many calculated properties to the complete basis set limit. This means that a significant part of the computational cost in many-electron perturbation theory calculations originates from the need to include large numbers of one-electron basis functions to achieve the desired level of precision. Many techniques have been developed to accelerate the convergence to the complete basis set limit including explicitly correlated methods, transcorrelated methods and focal-point approaches [1–17]. More recently, a density-functional theory based approach has also been employed to correct for basis set incompleteness errors [18]. Furthermore, there exist a wide range of techniques that aim at extrapolating to the complete basis set limit [19–21].

Explicitly correlated methods are undeniably among the most reliable and efficient methods to correct for the basis set incompleteness error (BSIE) in quantum chemical many-electron theories. They account for the first-order cusp condition in the many-electron wavefunction ansatz explicitly and are commonly referred to as F12 theories, where F12 stands for a two-electron correlation factor that enables a compact expansion of the wavefunction at short interelectronic distances [1–6]. Despite the need for additional many-electron integrals such as three- and sometimes even four-electron integrals, explic-

itly correlated coupled-cluster theories have been implemented in a computationally efficient manner, allowing for numerically stable and precise *ab initio* calculations of molecular systems [1, 2, 5, 22–28].

Focal-point approaches seek to combine low and high-level theories in a computationally efficient manner to correct for the BSIE in the high-level calculation. In this work we seek to correct for the BSIE of coupled-cluster theory using corrections based on second-order Møller-Plesset perturbation theory (MP2). Unfortunately, the BSIEs of MP2 and coupled-cluster singles and doubles (CCSD) energies usually differ significantly. This can be attributed to the so-called “interference effect” that leads to a reduction in the BSIE of CCSD theory compared to MP2 theory [29, 30]. Peterson *et al.* account for this effect using complete basis set (CBS) limit model chemistry via an empirical formula [31]. Similar approaches include rescaled explicitly correlated MP2 energies [32]. We stress that the particle-particle ladder (PPL) contribution to the CCSD correlation energy is the leading cause of the interference effect. Therefore, its contribution to the BSIE needs to be treated as accurately as possible to attain well converged CCSD energies [33–35]. In this context, it is noteworthy that studies on the basis set convergence in third-order perturbation theory have also revealed the significance of corresponding PPL contributions [36, 37].

Recently, we have explored a focal-point approach to correct for the BSIE of CCSD correlation energies that is based on its diagrammatic decomposition into an MP2, PPL and so-called rest term [34]. The decomposition of the CCSD correlation energy into contributions that dominate the BSIE (MP2 and PPL) and the rest can be very useful in *ab initio* calculations for the following two reasons. Firstly, the MP2 correlation energy in the com-

* andreas.irmler@tuwien.ac.at

plete basis set limit can be computed using algorithms with low computational complexity, removing the corresponding BSIE almost exactly [38–41]. Secondly, constructing approximations to the BSIE in the PPL term is a much simpler challenge than correcting the BSIE in all possible diagrammatic contributions to the CCSD correlation energy. Furthermore, the MP2 and PPL terms can be regarded as an independent electron pair approximation to CCSD theory, which simplifies the development of an electron pair-specific BSIE correction. In Ref. [35] we have shown that even a simple correction to the PPL BSIE, that is based on rescaling a corresponding MP2 correction, achieves significant reductions in the BSIE of the CCSD correlation energy. However, the attained level of precision did not reach F12-like quality for all investigated properties.

Here, we present a computationally efficient and significantly more accurate method to correct for the BSIE in the PPL term of the CCSD correlation energy. Compared to our previous work in Ref. [35], the improvements result from the following two modifications. Firstly, we employ frozen natural orbitals for the virtual orbital manifold calculated from approximate one-particle reduced density matrices [42]. Secondly, and most importantly, we introduce approximations to the electron pair wavefunctions appearing in the expression for the PPL term, making it possible to compute BSIE corrections with low computational cost but high accuracy. To this end, we develop a pair-specific mean-field ansatz that exhibits an average correlation hole depth that agrees with the spatially averaged correlation hole depth of the coupled-cluster or first-order wavefunction in a finite basis set. Employing this mean-field ansatz in the bra or ket state of the PPL expression leads to considerable simplifications. The derived pair-specific BSIE correction effectively corresponds to the rescaled MP2 BSIE. As already mentioned above, the scaling factor depends on averaged correlation hole depths. In hindsight, our work corroborates the success of CCSD basis set corrections that are based on rescaling MP2 BSIEs. We note that the averaged pair-specific correlation hole depth can be computed from the electronic transition structure factor, which introduces the need for two-electron integrals employing the $\delta(\mathbf{r}_{12})$ -kernel. However, these additional integrals do not increase significantly the computational complexity of a conventional MP2 calculation in a finite basis set. We demonstrate that the introduced BSIE correction yields CCSD correlation energies that converge rapidly with respect to the number of frozen natural orbitals.

II. THEORY

A. The pair-specific decomposed PPL correlation energy in the CBS limit

In this work we introduce a correction to the BSIE of the CCSD correlation energy. The CCSD correlation

energy is given by

$$E_c^{\text{CCSD}} = \sum_{ij} \sum_{ab} T_{ij}^{ab} (2 \langle ij|V|ab \rangle - \langle ji|V|ab \rangle) \quad (1)$$

and can be decomposed into different diagrammatic contributions such that [34]

$$E_c^{\text{CCSD}} = E^{\text{mp2}} + E^{\text{ppl}} + \underbrace{E^{\text{phl}} + E^{\text{hhl}} + E^{\text{phr}} + \dots}_{E^{\text{rest}}}, \quad (2)$$

where E^{mp2} corresponds to the MP2 correlation energy

$$E^{\text{mp2}} = \sum_{ij} \sum_{ab} W_{ab}^{ij} \langle ab|V|ij \rangle \quad (3)$$

and the particle-particle ladder term is defined as

$$E^{\text{ppl}} = \sum_{ij} \sum_{ab} W_{ab}^{ij} \sum_{cd} \langle ab|V|cd \rangle T_{ij}^{cd}. \quad (4)$$

We note that E^{mp2} was referred to as E^{driver} in previous related work [34, 43]. T_{ij}^{cd} is computed from the CCSD singles (t_i^a) and doubles (t_{ij}^{ab}) amplitudes as $T_{ij}^{ab} = t_{ij}^{ab} + t_i^a t_j^b$. t_i^a and t_{ij}^{ab} are obtained by solving the corresponding amplitude equations [44, 45]. W_{ab}^{ij} is given by

$$W_{ab}^{ij} = \frac{2 \langle ij|V|ab \rangle - \langle ji|V|ab \rangle}{\epsilon_i + \epsilon_j - \epsilon_a - \epsilon_b}. \quad (5)$$

All equations refer to spin-restricted spatial orbitals with the Coulomb integrals defined by

$$\langle ij|V|ab \rangle = \iint d\mathbf{r}_1 d\mathbf{r}_2 \phi_i^*(\mathbf{r}_1) \phi_j^*(\mathbf{r}_2) v(r_{12}) \phi_a(\mathbf{r}_1) \phi_b(\mathbf{r}_2), \quad (6)$$

using the Coulomb kernel $v(r_{12}) = 1/|\mathbf{r}_1 - \mathbf{r}_2|$.

The following discussion is based on the premise that the finite virtual orbital manifold is spanned by a set of canonical orbitals that needs to be augmented with additional virtual orbitals to reach the CBS limit, while the occupied orbitals are fully converged to the CBS limit regardless of the approximations used in the virtual orbital space. This situation closely resembles *ab initio* calculations employing re-canonicalized frozen natural orbitals [42]. We choose the following index labels for occupied and virtual spatial orbitals

$$\begin{aligned} i, j, k, \dots & \text{occupied states} \\ a, b, c, \dots & \text{virtual states in finite basis} \\ \alpha, \beta, \gamma, \dots & \text{augmented virtual states} \\ A, B, C, \dots & \text{union of all virtual states.} \end{aligned}$$

The particle-particle ladder term (E^{ppl}) defined by Eq. (4) can also be expressed as

$$\epsilon_{ij}^A = \langle \Psi_{ij}^{(1)} | V | \Psi_{ij}^{\text{cc}} \rangle, \quad (7)$$

where

$$\langle \Psi_{ij}^{(1)} | = \sum_{ab} W_{ab}^{ij} \langle ab |, \quad (8)$$

and

$$|\Psi_{ij}^{cc}\rangle = \sum_{cd} T_{ij}^{cd} |cd\rangle. \quad (9)$$

Herein $|\Psi_{ij}^{(1)}\rangle$ refers to the linearized first order wavefunction whereas $|\Psi_{ij}^{cc}\rangle$ resembles a coupled-cluster pair wavefunction. Consequently, the PPL term only couples wavefunctions with the same occupied pair index.

We formally define the CBS limit of the linearized first-order and coupled-cluster-like pair wavefunction by

$$|\Psi_{ij}^{(1)\text{-cbs}}\rangle = |\Psi_{ij}^{(1)}\rangle + |\delta_{ij}^{(1)}\rangle \quad (10)$$

and

$$|\Psi_{ij}^{cc\text{-cbs}}\rangle = |\Psi_{ij}^{cc}\rangle + |\delta_{ij}^{cc}\rangle, \quad (11)$$

respectively. $|\delta_{ij}^{(1)}\rangle$ and $|\delta_{ij}^{cc}\rangle$ are defined such that they correct for the BSIE in the respective parent wavefunctions $|\Psi_{ij}^{(1)}\rangle$ and $|\Psi_{ij}^{cc}\rangle$. Already in 1985, Kutzelnigg discussed that the conventional expansion, using products of one-electron states, can not represent the wavefunction accurately at regions where the interelectronic distance approaches zero [46]. Thus, for increasing one-electron basis set sizes, the contribution of $|\delta_{ij}^{(1)}\rangle$ and $|\delta_{ij}^{cc}\rangle$ will largely be localized to the cusp region at small interelectronic distances. Substituting the above BSIE corrections into Eq. (7), yields the following contributions to the PPL energy in the CBS limit:

$$\epsilon_{ij}^B = \langle \delta_{ij}^{(1)} | V | \Psi_{ij}^{cc} \rangle \quad (12)$$

$$\epsilon_{ij}^C = \langle \Psi_{ij}^{(1)} | V | \delta_{ij}^{cc} \rangle \quad (13)$$

$$\epsilon_{ij}^D = \langle \delta_{ij}^{(1)} | V | \delta_{ij}^{cc} \rangle. \quad (14)$$

Consequently, the CBS limit formally reads

$$E^{\text{ppl-cbs}} = \sum_{ij} (\epsilon_{ij}^A + \epsilon_{ij}^B + \epsilon_{ij}^C + \epsilon_{ij}^D). \quad (15)$$

This work outlines an efficient approximation to $E^{\text{ppl-cbs}}$. To this end, we analyze ϵ_{ij}^B and ϵ_{ij}^C and provide suitable approximations for them in the following sections. We disregard ϵ_{ij}^D since it is of second order in the BSIE of the pair wavefunctions (δ). We recall that ϵ_{ij}^A is evaluated in the conventional coupled-cluster calculation using the finite basis set.

B. Coupling of $|\delta_{ij}^{(1)}\rangle$ to $|\Psi_{ij}^{cc}\rangle$

We now turn to the expression for ϵ_{ij}^B and employ the resolution of the identity (RI)

$$\begin{aligned} \epsilon_{ij}^B &= \sum_{\alpha\beta} \langle \delta_{ij}^{(1)} | \alpha\beta \rangle \langle \alpha\beta | V | \Psi_{ij}^{cc} \rangle \\ &+ \sum_{a\beta} \langle \delta_{ij}^{(1)} | a\beta \rangle \langle a\beta | V | \Psi_{ij}^{cc} \rangle \\ &+ \sum_{\alpha b} \langle \delta_{ij}^{(1)} | \alpha b \rangle \langle \alpha b | V | \Psi_{ij}^{cc} \rangle. \end{aligned} \quad (16)$$

The above equation can be interpreted as the coupling of the change of the first-order wavefunction to $|\Psi_{ij}^{cc}\rangle$. Due to $\langle \delta_{ij}^{(1)} | ab \rangle = 0$, only projectors that involve at least one state from the augmented virtual basis have to be included in the RI. The orbitals ϕ_α , and ϕ_β are strongly oscillating in space, *i.e.*, they bear large wave number and/or high angular momentum number. In contrast, $|\Psi_{ij}^{cc}\rangle$ is expected to be much smoother. Following fundamental ideas of scattering theory, we replace the complicated scattering problem with a much simpler one, by means of the following approximation

$$|\Psi_{ij}^{cc}\rangle = \sum_{cd} T_{ij}^{cd} |cd\rangle \approx |ij\rangle g_{ij}^{cc}, \quad (17)$$

where $|ij\rangle$ is a mean-field state constructed from the Hartree–Fock orbitals of the occupied pair i and j . The scaling factor g_{ij}^{cc} is chosen such that the spatially averaged correlation hole depths of the correlated wavefunction and its mean-field approximation are equated after projection onto the occupied space of the same electron pair:

$$\sum_{cd} T_{ij}^{cd} \langle ij | \delta(\mathbf{r}_{12}) | cd \rangle = \langle ij | \delta(\mathbf{r}_{12}) | ij \rangle g_{ij}^{cc}. \quad (18)$$

The appearing integrals are defined in an analogous manner to Eq. (6) but with the Coulomb kernel replaced by the Dirac delta function $\delta(\mathbf{r}_{12})$. When using Gaussian basis functions, this requires only minor modifications of the original integral routines (see [47]). From the above equation, we obtain an explicit expression for the pair-specific correlation hole depth scaling factor given by

$$g_{ij}^{cc} = \frac{\sum_{cd} T_{ij}^{cd} \langle ij | \delta(\mathbf{r}_{12}) | cd \rangle}{\langle ij | \delta(\mathbf{r}_{12}) | ij \rangle}. \quad (19)$$

For the sake of brevity in the following paragraphs, we introduce a projection operator \hat{g}_{ij} that yields an approximate mean-field state when applied to any correlated electron pair state, such that

$$|ij\rangle g_{ij}^{cc} = \hat{g}_{ij} |\Psi_{ij}^{cc}\rangle. \quad (20)$$

To get a better understanding of the above approximation, we now inspect the explicit expression for ϵ^B of

a singlet state, which is given by

$$\langle \delta | V | \psi \rangle = \iint d\mathbf{r}_{12} d\bar{\mathbf{r}}_{12} \tilde{\delta}^*(\mathbf{r}_{12}, \bar{\mathbf{r}}_{12}) \frac{1}{|\mathbf{r}_{12}|} \tilde{\psi}(\mathbf{r}_{12}, \bar{\mathbf{r}}_{12}). \quad (21)$$

Here, the electron-pair functions δ and ψ have been transformed to a real-space representation in $\mathbf{r}_{12} = \mathbf{r}_1 - \mathbf{r}_2$ and $\bar{\mathbf{r}}_{12} = \mathbf{r}_1 + \mathbf{r}_2$. Because $\tilde{\delta}$ is largely localized around the cusp region, it effectively screens the Coulomb kernel at large interelectronic distances $|\mathbf{r}_{12}|$. ϵ^B is therefore dominated by contributions from short interelectronic distances. Moreover, $\tilde{\psi}$ is a smooth function in the cusp region compared to $\tilde{\delta}$, suggesting that

$$\tilde{\psi}(\mathbf{r}_{12}, \bar{\mathbf{r}}_{12}) \approx \tilde{\psi}(\mathbf{r}_{12} = 0, \bar{\mathbf{r}}_{12}) \quad (22)$$

is a reasonable approximation. $\tilde{\psi}(0, \bar{\mathbf{r}}_{12})$ is the correlation hole depth as a function of $\bar{\mathbf{r}}_{12}$. The central approximation of this work is based on employing a mean field ansatz for $\tilde{\psi}(0, \bar{\mathbf{r}}_{12})$ that is obtained by projecting $\tilde{\psi}(0, \bar{\mathbf{r}}_{12})$ onto a corresponding zeroth-order mean-field wave function and ensuring that the spatially averaged correlation depths of the mean-field ansatz and $\tilde{\psi}$ agree. This is achieved using the pair-specific projection operator \hat{g}_{ij} defined in Eq. (20).

Using the mean-field approximation described above, ϵ_{ij}^B can be approximated as follows

$$\epsilon_{ij}^B = \langle \delta_{ij}^{(1)} | V | \Psi_{ij}^{cc} \rangle \approx \underbrace{\langle \delta_{ij}^{(1)} | V | ij \rangle}_{\Delta\epsilon_{ij}^{(2)}} g_{ij}^{cc} \quad (23)$$

where $\Delta\epsilon_{ij}^{(2)}$ refers to the pair-specific BSIE correction of the MP2 correlation energy. Thus, we have shown that the ϵ_{ij}^B contribution to the PPL term can be approximated using $\Delta\epsilon_{ij}^{(2)}$ times a scaling factor that depends on the spatially averaged correlation hole depth of $|\Psi_{ij}^{cc}\rangle$.

C. Coupling of $|\delta_{ij}^{cc}\rangle$ to $|\Psi_{ij}^{(1)}\rangle$

We now focus on the coupling between the first-order wavefunction and the BSIE correction to Ψ_{ij}^{cc} . Using once more the RI we write Eq. (13) in the following way

$$\begin{aligned} \epsilon_{ij}^C &= \sum_{CD} \langle \Psi_{ij}^{(1)} | V | CD \rangle \langle CD | \delta_{ij}^{cc} \rangle \\ &\approx \sum_{CD} \langle \Psi_{ij}^{(1)} | \hat{g}_{ij}^\dagger V | CD \rangle \langle CD | \delta_{ij}^{cc} \rangle \\ &= g_{ij}^{(1)} \sum_{CD} \langle ij | V | CD \rangle \langle CD | \delta_{ij}^{cc} \rangle. \end{aligned} \quad (24)$$

In the above equation, we have approximated the first-order state by a mean-field state that exhibits an identical spatially averaged correlation hole depth. Furthermore, the exact expression for $|\delta_{ij}^{cc}\rangle$ is not accessible, as we do

not intend to solve the coupled-cluster equations in the large basis set. Moreover, we note that $\langle cd | \delta_{ij}^{cc} \rangle \neq 0$, which is in contrast to the BSIE of the first-order state, where $\langle cd | \delta_{ij}^{(1)} \rangle = 0$. Therefore, we approximate the orbital representation of $|\delta_{ij}^{cc}\rangle$ including only the dominant contributions (driver and PPL) in the complete basis set limit of the amplitude equations:

$$\begin{aligned} \langle CD | \delta_{ij}^{cc} \rangle &\approx \underbrace{\langle CD | \delta_{ij}^{(1)} \rangle}_{(I)} \oplus \underbrace{\frac{\langle \gamma \zeta | V | \Psi_{ij}^{cc} \rangle}{\epsilon_i + \epsilon_j - \epsilon_\gamma - \epsilon_\zeta}}_{(II)} \\ &\oplus \underbrace{\frac{\langle C \zeta | V | \Psi_{ij}^{cc} \rangle}{\epsilon_i + \epsilon_j - \epsilon_C - \epsilon_\zeta}}_{(III)} \oplus \underbrace{\frac{\langle \gamma D | V | \Psi_{ij}^{cc} \rangle}{\epsilon_i + \epsilon_j - \epsilon_\gamma - \epsilon_D}}_{(IV)} \\ &\oplus \frac{\langle CD | V | \delta_{ij}^{cc} \rangle}{\epsilon_i + \epsilon_j - \epsilon_C - \epsilon_D} \oplus \dots \end{aligned} \quad (25)$$

The direct sum notation is used to emphasize the fact that γ is a subset of C . In the following we consider only those terms defined by (I) – (IV) because they are of zeroth-order in δV , while the rest is $\mathcal{O}(\delta V)$. We now turn to the contributions of the terms defined by (I) – (IV) to ϵ_{ij}^C . Inserting (I) from Eq. (25) into the last line of Eq. (24) yields

$$\epsilon_{ij}^C(I) = g_{ij}^{(1)} \Delta\epsilon_{ij}^{(2)}. \quad (26)$$

To account for the contributions of (II) – (IV) to ϵ_{ij}^C , we again approximate $|\Psi_{ij}^{cc}\rangle$ using the mean-field ansatz defined by Eq. (20). Inserting the resulting approximations into the last line of Eq. (24) yields

$$\epsilon_{ij}^C(II - IV) = g_{ij}^{(1)} \Delta\epsilon_{ij}^{(2)} g_{ij}^{cc}. \quad (27)$$

Therefore, our final approximation to Eq. (13) is given by

$$\epsilon_{ij}^C \approx \epsilon_{ij}^C(I) + \epsilon_{ij}^C(II - IV) = \Delta\epsilon_{ij}^{(2)} (g_{ij}^{(1)} + g_{ij}^{(1)} g_{ij}^{cc}), \quad (28)$$

which corresponds again to $\Delta\epsilon_{ij}^{(2)}$ scaled by a factor that depends on the correlation hole depths of $|\Psi_{ij}^{cc}\rangle$ and $|\Psi_{ij}^{(1)}\rangle$.

We note that a corresponding BSIE correction in MP3 theory would have to include $\epsilon_{ij}^C(I)$ only. However, in CCSD theory the BSIE of $|\Psi_{ij}^{cc}\rangle$ is not well approximated using $\delta_{ij}^{(1)}$. Therefore $\epsilon_{ij}^C(II - IV)$ accounts for the change of $\delta_{ij}^{(1)}$ due to the most important PPL coupling terms linear in $|\Psi_{ij}^{cc}\rangle$. The coupling strength of these terms is on the order of g_{ij}^{cc} and needs to be included to attain high accuracy.

D. The pair-specific PPL basis-set correction

We now summarize the final approximation to the BSIE correction of the PPL energy:

$$\epsilon_{ij}^B + \epsilon_{ij}^C \approx \Delta\epsilon_{ij}^{(2)}(g_{ij}^{cc} + g_{ij}^{(1)} + g_{ij}^{(1)}g_{ij}^{cc}). \quad (29)$$

We stress that the contribution of ϵ_{ij}^D defined in Eq. (14) has been neglected because it is not of leading order in δ . We arrive at the following approximate CBS limit expression of the PPL energy:

$$E^{\text{ps-ppl}} = E^{\text{ppl}} + \underbrace{\sum_{ij} \Delta\epsilon_{ij}^{(2)}(g_{ij}^{cc} + g_{ij}^{(1)} + g_{ij}^{(1)}g_{ij}^{cc})}_{\Delta_{\text{ps-ppl}}}. \quad (30)$$

At this point, we note again that in the above expression the pair-specific correlation hole depth scaling factors g_{ij}^{cc} and $g_{ij}^{(1)}$ are computed in a finite basis set, whereas $\Delta\epsilon_{ij}^{(2)}$ refers to the BSIE correction of the pair-specific MP2 correlation energy.

III. THE UNIFORM TWO ELECTRON GAS

In order to assess the presented approximations, we first study a particularly simple model system - the three-dimensional uniform electron gas (UEG). The details of this model are described for instance in Ref. [43]. For the here performed analysis it is enough to study only two electrons in a homogeneous positive background. The singlet ground state Hartree–Fock (HF) wave function is a constant function and the virtual HF states are plane-waves

$$\phi_a(\mathbf{r}) = \frac{1}{\sqrt{\Omega}} e^{i\mathbf{k}_a \cdot \mathbf{r}}, \quad (31)$$

with HF eigenvalues

$$\epsilon_a = \frac{1}{2} \mathbf{k}_a^2 - \frac{4\pi}{\Omega \mathbf{k}_a^2}. \quad (32)$$

Notice that the eigenenergies are ordered with respect to the length of the corresponding momentum vector. The unit cell volume is given by Ω . This simplifies the four-index integrals to

$$\langle ii|V|ab \rangle = \frac{4\pi}{\Omega |\mathbf{k}_a|^2} \delta_{\mathbf{k}_a + \mathbf{k}_b, 0}. \quad (33)$$

Consequently, the MP2 energy expression contains only a single sum

$$E^{\text{mp2}} = \sum_a \frac{\langle ii|V|a\bar{a} \rangle}{\epsilon_i + \epsilon_i - \epsilon_a - \epsilon_{\bar{a}}} \langle a\bar{a}|V|ii \rangle. \quad (34)$$

We use the notation \bar{a} for the virtual orbital with momentum vector $-\mathbf{k}_a$. The PPL energy expression reads

$$E^{\text{ppl}} = \sum_a \frac{\langle ii|V|a\bar{a} \rangle}{\epsilon_i + \epsilon_i - \epsilon_a - \epsilon_{\bar{a}}} \sum_c \langle a\bar{a}|V|c\bar{c} \rangle t_{ii}^{c\bar{c}}. \quad (35)$$

In a finite basis set calculation the number of virtual basis functions N_v has to be truncated. For the UEG model system, this is typically done by introducing a cutoff wave vector k_1 and considering only virtual states with $|\mathbf{k}_a| < k_1$. Following the ideas of section II, we introduce a second cutoff k_2 specifying the augmented virtual states α , with $k_1 \leq |\mathbf{k}_\alpha| < k_2$. Hence, we can write the following four contributions to the total PPL energy

$$\begin{aligned} \epsilon_{ii}^A &= \sum_a \frac{\langle ii|V|a\bar{a} \rangle}{\epsilon_i + \epsilon_i - \epsilon_a - \epsilon_{\bar{a}}} \sum_c \langle a\bar{a}|V|c\bar{c} \rangle t_{ii}^{c\bar{c}} \\ \epsilon_{ii}^B &= \sum_\alpha \frac{\langle ii|V|\alpha\bar{\alpha} \rangle}{\epsilon_i + \epsilon_i - \epsilon_\alpha - \epsilon_{\bar{\alpha}}} \sum_c \langle \alpha\bar{\alpha}|V|c\bar{c} \rangle t_{ii}^{c\bar{c}} \\ \epsilon_{ii}^C &= \sum_a \frac{\langle ii|V|a\bar{a} \rangle}{\epsilon_i + \epsilon_i - \epsilon_a - \epsilon_{\bar{a}}} \sum_\gamma \langle a\bar{a}|V|\gamma\bar{\gamma} \rangle t_{ii}^{\gamma\bar{\gamma}} \\ \epsilon_{ii}^D &= \sum_\alpha \frac{\langle ii|V|\alpha\bar{\alpha} \rangle}{\epsilon_i + \epsilon_i - \epsilon_\alpha - \epsilon_{\bar{\alpha}}} \sum_\gamma \langle \alpha\bar{\alpha}|V|\gamma\bar{\gamma} \rangle t_{ii}^{\gamma\bar{\gamma}}. \end{aligned} \quad (36)$$

We stress that one important feature of the UEG model consists in the fact, that enlarging the basis set does not alter the occupied and virtual orbitals. We now examine the proposed approximations numerically. We choose the union of all virtual states to be a very large number of 30046 states, which can be considered a good approximation to the CBS limit for the present system. In the following we gradually increase the number of virtual states in the finite basis and evaluate the approximate expressions for ϵ_{ii}^B and ϵ_{ii}^C in Eqs. (23) and (28) and compare them to the exact result in Eq. (36). The results for increasing numbers of virtual states are given in Table I. The contribution of ϵ_{ii}^B is roughly twice as large as ϵ_{ii}^C . We find that both energy contributions can be approximated with remarkable accuracy using the presented expressions. Although the approximations made for ϵ_{ii}^B and ϵ_{ii}^C differ, we can not observe any significant differences in the accuracy of both terms. The term ϵ_{ii}^D , for which no approximation was introduced, converges considerably faster, when compared to the other two contributions ϵ_{ii}^B and ϵ_{ii}^C . Hence, the BSIE of the PPL contribution can be reduced by a large portion successfully. It appears that the remaining deviation is roughly in the same order of magnitude as the rest contribution. Therefore, it is a reasonable approximation to neglect both contributions from ϵ_{ii}^D and ΔE^{rest} .

For the above analysis, we have employed the fully converged CCSD amplitudes expanded in a basis of 30046 virtual states. The amplitudes have been partitioned according to the cutoff k_1 into sets corresponding to $t_{ii}^{\alpha\bar{\alpha}}$ and $t_{ii}^{a\bar{a}}$, which have been used to compute ϵ_{ii}^B and ϵ_{ii}^C . However, in practice and for the following benchmark systems, we employ only CCSD amplitudes that have been calculated using a finite virtual orbital basis set.

TABLE I. BSIEs for the two-electron UEG with $r_s = 3.5$ a.u.. Reference energies are obtained from a calculation with 30046 virtals. Referred to exact (ex.) is the evaluation of Eq. (36) for the converged amplitudes using 30046 virtals and using N_v orbitals in the finite basis. Estimates (est.) are evaluated using Eqs. (23) and (28). The BSIE of the rest term is given in the last column and calculated between results obtained with N_v and 30046 virtual orbitals. All energies are given in mH.

| N_v | ϵ^B | | ϵ^C | | ϵ^D | ΔE^{rest} |
|-------|--------------|-------|--------------|-------|--------------|--------------------------|
| | ex. | est. | ex. | est. | ex. | |
| 26 | 0.582 | 0.560 | 0.255 | 0.262 | 0.178 | -0.065 |
| 56 | 0.343 | 0.332 | 0.157 | 0.162 | 0.076 | -0.049 |
| 122 | 0.171 | 0.166 | 0.079 | 0.083 | 0.027 | -0.029 |
| 250 | 0.087 | 0.084 | 0.047 | 0.043 | 0.010 | -0.015 |
| 514 | 0.043 | 0.043 | 0.021 | 0.022 | 0.004 | -0.008 |

IV. COMPUTATIONAL DETAILS

In the following sections we present results obtained for a set of benchmark systems including 107 molecules and atoms. We employ aug-cc-pVXZ basis sets for first-row elements and aug-cc-pV(X+d)Z basis sets for second-row elements [48, 49]. These basis sets will be denoted as AVXZ throughout this work. We obtained the reference energies using the quantum chemistry package PSI4 [50]. We have modified the code such that the E^{pp1} contribution is extracted from the calculation as described in Ref. [35]. For the CBS limit estimates we use AV5Z and AV6Z energies and the extrapolation formula $E_X = E_{\text{CBS}} + a/X^3$, with the basis set cardinal number X . This formula is used to get CBS estimates of all three individual terms: E^{mp2} , E^{pp1} , and E^{rest} . We use unrestricted Hartree–Fock orbital functions and corresponding CCSD implementations for all open-shell systems. All correlation energy calculations in this work used the frozen core approximation.

In addition, (F12*) calculations are performed using TURBOMOLE [51–54] and the AVDZ, AVTZ, and AVQZ basis sets. We employ default settings, however, we use the RI basis aug-cc-pV5Z developed by Hättig [55] in all calculations. We note that these large RI basis sets are employed for all types of auxiliary functions in the TURBOMOLE implementation, *i.e.* \$cbas, \$jkbas, and \$cabs. All results in the main text employ $\gamma = 1.0$ in the parametrization of the correlation factor. Further results using a different γ parameter can be found in the supplement information.

The derived approximate BSIE corrections to the PPL term were obtained using our own coupled-cluster code cc4s, LIBINT2 [56] and CTF [57]. In these calculations, the Hartree–Fock ground state wave function was obtained with the NWChem package [58] and interfaced to cc4s as described in Ref. [59]. We note that the introduced basis set correction scheme requires consistent sets of occupied orbitals for varying basis sets. However, this is not automatically guaranteed for degenerate sets of occupied orbitals. In this work, we avoid arbitrary unitary rotations among degenerate sets of orbitals by introducing point charges far away from the molecules and atoms that break corresponding symmetries, lifting all possibly

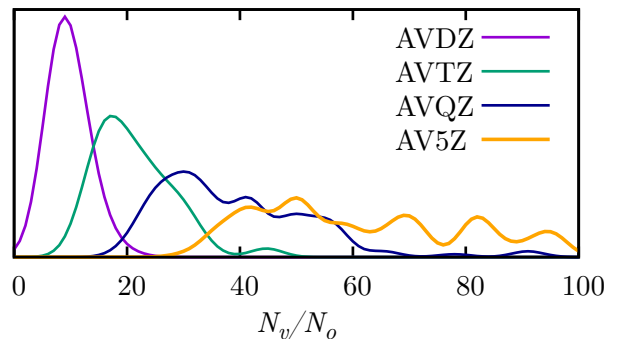


FIG. 1. Distribution of the number of virtual orbitals per occupied orbital for all 107 studied systems when employing an atom-centered AVXZ basis set. The same Gaussian function was used to smear the data points.

problematic degeneracies. These point charges are sufficiently far away to ensure that all computed correlation energies change by a numerically negligible small amount.

For the newly introduced basis set correction scheme we construct frozen natural orbitals (FNOs) on the level of second-order perturbation theory [42, 60, 61]. We truncate the virtual space used for the CCSD calculations by choosing only N_v FNOs with the largest occupation number, where $N_v = X_{\text{no}} \times \max(N_{o,\alpha}, N_{o,\beta})$ with $X_{\text{no}} \in [12, 16, 20, 24, 28, 32]$. $N_{o,\alpha}$ and $N_{o,\beta}$ refer to the number of occupied spin-up and spin-down orbitals, respectively. We stress that we use large basis sets (AVQZ and AV5Z) for the construction of FNOs. Therefore, the number of virtual orbitals, N_v , is defined differently than for conventional quantum chemical calculations. In conventional calculations with atom-centered basis sets, the total number of orbitals is independent of the number of occupied orbitals but depends only on the atomic species for a chosen basis set. Yet, we seek to compare the BSIEs of correlation energies calculated using both approaches. To provide an estimate for which cardinal number in the AVXZ basis set family corresponds on average to which number of virtual orbitals per occupied orbital, Fig. 1 depicts N_v/N_o for all studied atomic and molecular sys-

tems employing conventional AVXZ ($X=D,T,Q,5$) basis sets. We find that AVDZ and AVTZ roughly correspond to $X_{\text{no}} = 12$ and $X_{\text{no}} = 20$, respectively. Later, it will be numerically verified that our choice of fixed number of virtuals per occupied leads to a well-balanced energy description for different reactants.

We have calculated the correlation energies of in total 107 molecules and atoms. Thereupon we evaluated 26 closed-shell reaction energies (REc), 39 open-shell reaction energies (REo), 44 atomization energies (AE), 16 electron affinities (EA), and 22 ionization potentials (IP). This benchmark set is a subset of the one studied by Knizia *et al.* [5]. We had to exclude a number of molecules from their benchmark set as some of the molecules have been too large to be treated with our workflow. For some other molecules, we were not able to converge to a common HF ground state with neither of the three packages NWChem, TURBOMOLE, and PSI4. These molecules have also been excluded from our benchmark. A detailed list of the calculated molecules and corresponding reactions can be found in the supplement information.

V. RESULTS

This section presents results for molecular systems and is organized as follows. In section V A we assess the convergence of the diagrammatically decomposed CCSD correlation energy contributions, confirming that the BSIEs in the total energy are dominated by the MP2 and PPL terms. In section V B we show that this behavior persists for most quantities computed from the total energies including reaction energies, atomization energies, ionization potentials and electron attachment energies. In addition, we explore the accuracy of the derived approximate correction to the BSIE of the PPL term for all investigated quantities. In section V C we assess the accuracy of the corrected total CCSD energies and related quantities using two practical settings for the introduced focal-point approach and the respective BSIE corrections to the PPL term. The obtained results are compared to conventional CCSD and CCSD(F12*) approaches. Section V D discusses our findings for the (T) and (T*) correlation energy contributions using FNOs.

A. Total energies

We begin the analysis of the molecular systems by presenting results for the basis set errors of the diagrammatically decomposed correlation energy contributions for 107 molecules and atoms. Fig. 2 depicts the BSIEs of the PPL (ΔE^{PPL}), MP2 (ΔE^{MP2}) and rest (ΔE^{rest}) contributions. Furthermore, the BSIEs of the PPL energies corrected according to Eq.(30) are also depicted ($\Delta E^{\text{ps-PPL}}$). The BSIEs are estimated using reference values obtained from a [56] extrapolation. The corre-

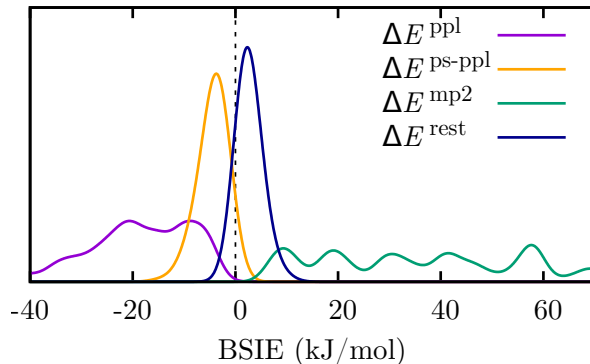


FIG. 2. Distribution of the basis set incompleteness error (BSIE) of various investigated energy channels (MP2, PPL and rest) including the corrected PPL energy ($\Delta E^{\text{ps-PPL}}$) for 107 studied systems. The energies were calculated using 16 frozen natural orbitals per occupied orbital and are referenced to [56] values. The same Gaussian function was used to smear the data points.

lation energies are evaluated using a Hartree-Fock reference wave function and 16 FNOs per occupied orbital to approximate the virtual orbital manifold. This basis set size is on average between AVDZ and AVTZ, as can be seen in Fig. 1. For the construction of the FNOs, the one-particle reduced density matrix was calculated in an AV5Z basis set. Our findings show that MP2 energies calculated using 16 FNOs per occupied orbital exhibit by far the largest BSIEs when compared to the other contributions. In contrast to MP2, E^{rest} is significantly better converged. This analysis reveals that E^{rest} can already be well approximated using a smaller number of natural orbitals than required for E^{PPL} and E^{MP2} . However, adding the basis set correction to E^{PPL} as defined in Eq.(30), significantly reduces the remaining BSIE such that $\Delta E^{\text{ps-PPL}}$ becomes comparable to ΔE^{rest} for all studied systems. This demonstrates impressively that the approximation derived in Sec. II can transfer its accuracy from the uniform electron gas model system to real atoms and molecules.

B. Energy differences

More decisive than well converged total energies is the question of how the proposed correction scheme works for energy differences. Therefore, we analyze the BSIEs for the different channels (E^{PPL} , E^{MP2} , and E^{rest}) for REc, REo, and AEs. The results are summarized in Table II for increasing numbers of FNOs as well as for the basis sets AVDZ-AV6Z. The MP2 contribution shows the largest BSIE followed by the PPL contribution. This is in accordance with the findings for the total energies, discussed in the previous section. We stress that only in the case of REc, the BSIE of E^{rest} and E^{PPL} is of comparable

TABLE II. BSIEs of correlation energy contributions to REc, REo and AEs. Shown are the rms deviations to the [56] reference. Results have been obtained using 12-32 FNOs per occupied orbitals (X_{no}), [23]-[45] extrapolations, and for different conventional basis sets ranging from AVDZ up to AV6Z.

| | ΔE^{mp2} | REc (kJ/mol) | | | $\Delta E^{\text{ps-pp1}}$ | ΔE^{mp2} | REo (kJ/mol) | | $\Delta E^{\text{ps-pp1}}$ | ΔE^{mp2} | AEs (kJ/mol) | | $\Delta E^{\text{ps-pp1}}$ |
|--------------------|-------------------------|-------------------------|--------------------------|-------|----------------------------|-------------------------|-------------------------|--------------------------|----------------------------|-------------------------|-------------------------|--------------------------|----------------------------|
| | | ΔE^{pp1} | ΔE^{rest} | | | | ΔE^{pp1} | ΔE^{rest} | | | ΔE^{pp1} | ΔE^{rest} | |
| $X_{\text{no}}=12$ | 6.396 | 1.850 | 1.212 | 1.199 | 28.325 | 8.811 | 1.513 | 1.986 | 39.350 | 14.985 | 2.783 | 2.257 | |
| $X_{\text{no}}=16$ | 4.576 | 1.302 | 0.822 | 0.931 | 20.556 | 6.509 | 0.783 | 1.502 | 28.230 | 11.118 | 1.437 | 1.321 | |
| $X_{\text{no}}=20$ | 2.978 | 0.877 | 0.437 | 0.739 | 15.771 | 5.224 | 0.489 | 1.390 | 22.094 | 8.941 | 1.005 | 0.949 | |
| $X_{\text{no}}=24$ | 2.240 | 0.540 | 0.338 | 0.667 | 12.429 | 4.130 | 0.308 | 1.257 | 17.231 | 7.115 | 0.650 | 0.723 | |
| $X_{\text{no}}=28$ | 2.289 | 0.626 | 0.299 | 0.536 | 9.416 | 3.114 | 0.242 | 1.284 | 14.024 | 5.930 | 0.600 | 0.664 | |
| $X_{\text{no}}=32$ | 2.476 | 0.649 | 0.516 | 0.485 | 7.241 | 2.398 | 0.392 | 1.325 | 11.494 | 4.903 | 0.559 | 0.627 | |
| AVDZ | 15.207 | 2.400 | 3.468 | - | 43.096 | 10.296 | 5.200 | - | 67.192 | 21.166 | 12.269 | - | |
| AVTZ | 6.981 | 1.767 | 2.040 | - | 20.598 | 5.675 | 2.544 | - | 27.203 | 9.567 | 4.153 | - | |
| AVQZ | 3.212 | 1.077 | 0.653 | - | 8.945 | 2.666 | 0.624 | - | 11.866 | 4.321 | 0.831 | - | |
| AV5Z | 1.885 | 0.640 | 0.288 | - | 4.553 | 1.370 | 0.300 | - | 6.122 | 2.257 | 0.274 | - | |
| AV6Z | 1.092 | 0.371 | 0.164 | - | 2.636 | 0.793 | 0.177 | - | 3.541 | 1.306 | 0.158 | - | |
| [23] | 5.420 | 1.708 | 2.049 | - | 11.576 | 3.901 | 2.852 | - | 11.131 | 4.941 | 2.534 | - | |
| [34] | 2.007 | 0.842 | 0.815 | - | 1.393 | 0.662 | 1.468 | - | 1.237 | 0.708 | 1.845 | - | |
| [45] | 0.730 | 0.262 | 0.148 | - | 0.719 | 0.237 | 0.400 | - | 0.458 | 0.172 | 0.416 | - | |

magnitude. Furthermore, we note that the computed errors using FNOs for some systems become larger again or do not reduce significantly for $X_{\text{no}} > 24$. We attribute this behavior to not sufficiently well converged FNOs. When approaching $X_{\text{no}} > 24$, one would require even bigger basis sets than the employed AV5Z for the construction of the FNOs. Generally, it is not expected that the errors are significantly smaller than when using all possible virtual orbitals in the AV5Z basis set.

Especially for the large basis sets, the BSIE of the rest contribution is remarkably small; the rms deviation for AV5Z is only around 0.3 kJ/mol and lower. A similar high accuracy can be attained when using only a comparably small number of 20 FNOs per occupied orbital, which achieves rms deviations of around 0.5 kJ/mol for the reaction energies and 1 kJ/mol for atomization energies.

For REo and AEs the PPL contribution converges significantly slower with respect to the basis set size compared to E^{rest} . Furthermore, the BSIE cannot be diminished considerably with a finite number of FNOs. This behavior changes when taking the proposed correction into account. Compared to the uncorrected PPL contribution, the BSIE of the corrected PPL contribution is reduced by a factor of four and more, when using only 20 FNOs per occupied or less. For REc the correction has no significant effect.

In summary, rms deviations of the rest contributions (ΔE^{rest}) and corrected PPL ($\Delta E^{\text{ps-pp1}}$) contributions are on the scale of 1 kJ/mol when using 20 FNOs per occupied orbital. Reaching a similar accuracy by employing conventional basis set calculations would require a [34] extrapolation.

C. Benchmarking a practical focal-point approach

Based on the findings in the previous sections we now define and assess a practical focal-point approach to compute total CCSD energies. For an even-tempered composition we combine extrapolated MP2 energies with CCSD calculations employing FNOs. We introduce the following two compositions:

$$\begin{aligned} E^{\text{FPa}} &= E^{\text{mp2}}([34]) + E^{\text{rest}}(12) + E^{\text{pp1}}(12) \\ &= E^{\text{ccsd}}(12) - E^{\text{mp2}}(12) + E^{\text{mp2}}([34]) \end{aligned} \quad (37)$$

and

$$\begin{aligned} E^{\text{FPb}} &= E^{\text{mp2}}([45]) + E^{\text{rest}}(20) + E^{\text{pp1}}(20) \\ &= E^{\text{ccsd}}(20) - E^{\text{mp2}}(20) + E^{\text{mp2}}([45]). \end{aligned} \quad (38)$$

$E^{\text{mp2}}(X_{\text{no}})$, $E^{\text{ccsd}}(X_{\text{no}})$, $E^{\text{rest}}(X_{\text{no}})$ and $E^{\text{pp1}}(X_{\text{no}})$ refer to the corresponding correlation energy contributions calculated employing X_{no} FNOs per occupied orbital. $E^{\text{mp2}}([34])$ and $E^{\text{mp2}}([45])$ refer to MP2 correlation energies obtained from a [34] and [45] extrapolation, respectively. For the first ansatz (E^{FPa}) we construct the FNOs using an AVQZ calculation, whereas for the second ansatz (E^{FPb}) the AV5Z basis set is used. In this section we will explore benchmark results obtained using both approaches with and without the introduced $\Delta_{\text{ps-pp1}}$ correction that depends on the respective pair-specific extrapolated MP2 energies and correlation hole depths. The corresponding BSIEs are summarized in Table III.

The uncorrected focal-point approaches E^{FPa} and E^{FPb} yield only satisfying BSIEs for the closed-shell reaction energies. Here, FPa achieves the quality of the [34] result, although the CCSD calculation is performed with a significantly smaller virtual space of only 12 FNOs per

TABLE III. CCSD valence correlation energy basis set incompleteness error for closed-shell reaction (REc), open-shell reactions (REo), atomization energies (AEs), ionization potentials (IPs), and electron affinities (EAs). Reference is obtained from a [56] extrapolation. Two different variants of the focal-point approximation are used with and without correction. Details are found in the main text.

| | REc (kJ/mol) | | REo (kJ/mol) | | AEs (kJ/mol) | | IPs (kJ/mol) | | EAs (kJ/mol) | |
|-------------------------------|--------------|-------|--------------|--------|--------------|--------|--------------|-------|--------------|-------|
| | max | rms | max | rms | max | rms | max | rms | max | rms |
| FPa | 4.823 | 1.905 | 15.403 | 7.130 | 24.223 | 11.786 | 10.244 | 3.301 | 15.384 | 5.414 |
| FPb | 2.828 | 1.029 | 10.998 | 5.445 | 16.660 | 8.461 | 6.837 | 2.652 | 9.203 | 3.766 |
| FPa+ $\Delta_{\text{ps-ppl}}$ | 7.248 | 2.541 | 8.836 | 3.024 | 9.017 | 2.400 | 3.359 | 1.520 | 5.666 | 1.603 |
| FPb+ $\Delta_{\text{ps-ppl}}$ | 3.253 | 1.102 | 2.424 | 1.049 | 3.491 | 0.848 | 1.475 | 0.733 | 3.062 | 0.828 |
| [23] | 15.637 | 5.814 | 33.638 | 10.460 | 26.000 | 8.443 | 8.814 | 4.366 | 6.170 | 3.033 |
| [34] | 6.222 | 2.031 | 4.545 | 1.938 | 3.965 | 1.874 | 1.993 | 0.828 | 1.772 | 0.895 |
| [45] | 1.137 | 0.438 | 1.864 | 0.650 | 1.302 | 0.532 | 0.213 | 0.112 | 0.181 | 0.113 |
| (F12*) @ AVDZ | 9.859 | 3.163 | 14.625 | 4.274 | 11.957 | 5.821 | 8.375 | 4.632 | 7.059 | 4.720 |
| (F12*) @ AVTZ | 3.838 | 1.434 | 5.946 | 1.657 | 3.834 | 1.520 | 2.685 | 1.393 | 1.810 | 1.189 |
| (F12*) @ AVQZ | 2.233 | 0.869 | 1.727 | 0.719 | 1.795 | 0.532 | 0.898 | 0.543 | 1.015 | 0.472 |

occupied orbital. For the open-shell reactions and other properties, the focal-point method performs significantly worse with rms deviations between 3-12 kJ/mol and a maximum error of around 25 kJ/mol.

The focal-point approaches including the $\Delta_{\text{ps-ppl}}$ correction yield significantly more consistent BSIEs for all studied energy differences. The rms deviations are 1.5-3 kJ/mol and around 1 kJ/mol for FPa and FPb, respectively. For the FPb+ $\Delta_{\text{ps-ppl}}$ approach the maximum deviation is below 4 kJ/mol for all considered reactions.

We note that for the closed-shell reactions the corrected focal-point results show larger rms deviations and larger maximum errors than the uncorrected variants. We attribute this to fortuitous error cancellation between the individual energy contributions to the CCSD correlation energy. This is only visible when the $\Delta_{\text{ps-ppl}}$ correction is insignificant as it is the case for the closed-shell reaction energies (see Sec. VB). Correcting for the BSIE in the PPL term, reduces this error compensation, causing slightly larger BSIEs for closed-shell reaction energies. However, the results for REc obtained including the $\Delta_{\text{ps-ppl}}$ correction are of comparable size to open-shell reactions and other properties.

The extrapolation using the AVDZ and AVTZ basis sets shows large maximum errors of up to 30 kJ/mol and the rms deviation ranges from 3 to 10 kJ/mol. The [34] extrapolation yields satisfying results with rms deviations of around 2 kJ/mol, for IPs and EAs already below 1 kJ/mol. Although the [45] extrapolation yields the best statistical results, a CCSD calculation with the large AV5Z basis set is only possible for small systems. We stress that more sophisticated extrapolation techniques were already tested for the original version of the employed benchmark set. Results can be found in the supplement of Ref. [5]. Knizia *et al.* conclude that “[...] in our benchmark set there are only few systems where using either extrapolation scheme makes a noteworthy difference“. Thus, the corrected FPa ansatz is to be preferred over [23] extrapolation and the corrected FPb seems to

be superior compared with the [34] extrapolation. We stress that in both cases larger HF and MP2 calculations have to be performed in order to obtain the final result.

For comparison, CCSD(F12*) results are also given for three different basis sets. The F12 results obtained using the AVQZ basis set reach almost the quality of the [45] extrapolation, with rms deviations well below 1 kJ/mol. For the (F12*)@AVTZ results, the rms deviations are only around 1.5 kJ/mol, whereas (F12*)@AVDZ yields results that show rms deviations with about 3-5 kJ/mol. We note that (F12*)@AVTZ yields results with smaller rms deviations than the [34] extrapolation. We note that the size of the virtual space in the CCSD calculation for (F12*)@AVDZ and FPa+ $\Delta_{\text{ps-ppl}}$ is similar. The same is true for (F12*)@AVTZ and FPb+ $\Delta_{\text{ps-ppl}}$. However, the FPa and FPb approaches require HF and MP2 calculations using the AVQZ and AV5Z basis sets, respectively. Therefore, the entire computational cost of the proposed focal-point approaches depends strongly on the efficiency of the employed HF and MP2 algorithms. Further statistical analysis of the test set using HF and conventional CCSD is provided in the supplementary information.

D. Perturbative triples contribution

Having assessed the introduced focal-point approach for the CCSD method, we now turn to the discussion of BSIEs in the perturbative triples contribution to the CCSD(T) energies calculated using FNOs. In addition to the conventional approach of computing the (T) contribution, we will also explore the (T*) approximation, which approximates the CBS limit of (T) by rescaling the finite basis set result with a factor estimated on the level of MP2 theory as outlined in Ref. [5]. In this work, the scaling factor corresponds to $E^{\text{mp2}}([45])/E^{\text{mp2}}(X_{\text{no}})$. The results are summarized in Table IV. The rms deviations for the AVDZ are 2-8 kJ/mol and even with the corrected values, denoted as (T*), the errors are within

TABLE IV. BSIE of the (T) contribution to closed-shell reaction (REc), open-shell reactions (REo), atomization energies (AEs), ionization potentials (IPs), and electron affinities (EAs). Shown are the rms deviations to the [56] reference.

| | REc (kJ/mol) | | REo (kJ/mol) | | AEs (kJ/mol) | | IPs (kJ/mol) | | EAs (kJ/mol) | |
|--------------------|--------------|-------|--------------|-------|--------------|-------|--------------|-------|--------------|-------|
| | (T) | (T*) | (T) | (T*) | (T) | (T*) | (T) | (T*) | (T) | (T*) |
| $X_{\text{no}}=12$ | 0.914 | 0.522 | 1.925 | 0.456 | 2.881 | 0.633 | 0.808 | 0.387 | 1.378 | 0.710 |
| $X_{\text{no}}=16$ | 0.583 | 0.385 | 1.175 | 0.316 | 1.765 | 0.350 | 0.522 | 0.252 | 0.877 | 0.415 |
| $X_{\text{no}}=20$ | 0.418 | 0.265 | 0.808 | 0.255 | 1.336 | 0.259 | 0.381 | 0.177 | 0.679 | 0.333 |
| $X_{\text{no}}=24$ | 0.292 | 0.203 | 0.616 | 0.227 | 0.989 | 0.236 | 0.298 | 0.122 | 0.506 | 0.207 |
| $X_{\text{no}}=28$ | 0.268 | 0.183 | 0.487 | 0.241 | 0.824 | 0.209 | 0.260 | 0.110 | 0.421 | 0.166 |
| $X_{\text{no}}=32$ | 0.206 | 0.233 | 0.397 | 0.244 | 0.699 | 0.192 | 0.223 | 0.092 | 0.364 | 0.129 |
| AVDZ | 1.976 | 3.231 | 5.176 | 3.216 | 8.176 | 2.826 | 3.139 | 2.364 | 4.330 | 2.676 |
| AVTZ | 1.055 | 0.823 | 1.485 | 0.997 | 2.165 | 0.450 | 0.862 | 0.432 | 1.275 | 0.566 |
| AVQZ | 0.509 | 0.269 | 0.667 | 0.433 | 0.913 | 0.153 | 0.366 | 0.185 | 0.571 | 0.277 |
| AV5Z | 0.270 | 0.135 | 0.303 | 0.231 | 0.425 | 0.087 | 0.179 | 0.088 | 0.296 | 0.151 |
| AV6Z | 0.157 | 0.078 | 0.191 | 0.134 | 0.246 | 0.049 | 0.103 | 0.050 | 0.171 | 0.087 |
| [23] | 0.888 | - | 0.705 | - | 0.570 | - | 0.232 | - | 0.170 | - |
| [34] | 0.255 | - | 0.188 | - | 0.133 | - | 0.066 | - | 0.121 | - |
| [45] | 0.035 | - | 0.088 | - | 0.093 | - | 0.024 | - | 0.040 | - |

the range of 2-3 kJ/mol. With increasing cardinal numbers the deviations reduce considerably. AVQZ results show deviations of up to 1 kJ/mol, reducing even further for the (T*) correction where they do not surpass 0.5 kJ/mol. As it is apparent from the presented data, the usage of FNOs together with the (T*) ansatz seems to be highly effective. Already 12 FNOs per occupied orbital suffice to reduce the rms deviations to 0.7 kJ/mol and lower. When using 20 FNOs instead, this deviation reduces smoothly below 0.35 kJ/mol. We stress that computing the (T*) scaling factor using a [56] extrapolation instead of [45] extrapolation has almost no effect (0.05 kJ/mol in the rms BSIEs).

Considering the findings for the BSIEs listed in Tabs. III and IV in combination, shows that it is possible to obtain CCSD(T) correlation energy estimates of REc, REo, AEs, IPs and EAs with a root mean square deviation from the CBS limit below 4 kJ/mol using 12 FNOs per occupied orbital only. Employing 20 FNOs per occupied orbital reduces the rms BSIE to around 1 kJ/mol for all computed energy differences. A detailed summary of all computed energies and BSIEs can be found in the supplement information.

VI. SUMMARY AND CONCLUSION

In this work we introduced a new CCSD basis set correction scheme that employs FNOs and exhibits an excellent trade-off between virtual orbital basis set size and remaining BSIE. The introduced correction aims at removing the BSIEs of the most important contributions to the CCSD correlation energy in the CBS limit originating from the MP2 and PPL terms. We stress that our approach is electron pair-specific. The presented results for reaction energies, atomization energies, ionization potentials and electron attachment energies exhibit a rapid

convergence with respect to the basis set size. Furthermore, we have shown that the CBS limit of the (T) contribution to the CCSD(T) energy can be approximated with a similar efficiency when employing FNOs and a rescaling procedure previously referred to as (T*) [5].

The introduced focal-point approach is an interesting alternative to conventional basis set truncation techniques that are based on cardinal numbers. FNOs give access to much more finely incremented basis set sizes, while maintaining a stable and rapid convergence of many properties to the CBS limit. We did not observe significant shell filling effects that might cause non-monotonic energy convergence with respect to the FNO basis set size. However, we note that the presented approach relies on the availability of computational efficient algorithms to compute MP2 energies and FNOs.

We stress that our approach is directly transferable to *ab initio* calculations employing pseudo potentials. This will be beneficial for solid state calculations in a plane wave basis set, which is one of the main motivations for this research. Most solid state calculations using coupled-cluster theory and plane-wave basis sets performed so far employ FNOs and the electronic transition structure factor needed to compute correlation hole depths is readily available [62–64]. Furthermore, we stress that the outlined basis set corrections will also be interesting to other many-electron theories, where similar interference effects play an important role, for instance, Auxiliary-Field Quantum Monte Carlo [65].

Finally, we note that the introduced basis set correction scheme is expected to work reliably in systems exhibiting correlation hole depths that vary strongly between different electron pairs. This includes situations where core-valence electron correlation effects play an important role.

VII. ACKNOWLEDGEMENTS

The authors thankfully acknowledge support and funding from the European Research Council (ERC) under

the European Unions Horizon 2020 research and innovation program (Grant Agreement No 715594). The computational results presented have been achieved in part using the Vienna Scientific Cluster (VSC).

-
- [1] L. Kong, F. A. Bischoff, and E. F. Valeev, *Chem. Rev.* **112**, 75 (2012).
- [2] C. Hättig, W. Klopper, A. Köhn, and D. P. Tew, *Chem. Rev.* **112**, 4 (2012).
- [3] H.-J. Werner, T. B. Adler, and F. R. Manby, *J. Chem. Phys.* **126**, 164102 (2007).
- [4] W. Kutzelnigg and W. Klopper, *J. Chem. Phys.* **94**, 1985 (1991).
- [5] G. Knizia, T. B. Adler, and H.-J. Werner, *J. Chem. Phys.* **130**, 054104 (2009).
- [6] A. Grüneis, S. Hirata, Y.-y. Ohnishi, and S. Ten-no, *J. Chem. Phys.* **146**, 080901 (2017).
- [7] S. F. Boys, N. C. Handy, and J. W. Linnett, *Proc. Roy. Soc. London Ser. A.* **309**, 209 (1969).
- [8] S. F. Boys, N. C. Handy, and J. W. Linnett, *Proc. Roy. Soc. London Ser. A.* **310**, 43 (1969).
- [9] A. J. Cohen, H. Luo, K. Guthier, W. Dobrautz, D. P. Tew, and A. Alavi, *J. Chem. Phys.* **151**, 061101 (2019).
- [10] S. Ten-no, *Chem. Phys. Lett.* **330**, 169 (2000).
- [11] A. L. L. East and W. D. Allen, *J. Chem. Phys.* **99**, 4638 (1993).
- [12] A. G. Császár, W. D. Allen, and H. F. Schaefer, *J. Chem. Phys.* **108**, 9751 (1998).
- [13] M. O. Sinnokrot, E. F. Valeev, and C. D. Sherrill, *J. Am. Chem. Soc.* **124**, 10887 (2002).
- [14] T. Takatani, E. G. Hohenstein, M. Malagoli, M. S. Marshall, and C. D. Sherrill, *J. Chem. Phys.* **132**, 144104 (2010).
- [15] P. Jurečka, J. Šponer, J. Černý, and P. Hobza, *Phys. Chem. Chem. Phys.* **8**, 1985 (2006).
- [16] C. E. Warden, D. G. A. Smith, L. A. Burns, U. Bozkaya, and C. D. Sherrill, *J. Chem. Phys.* **152**, 124109 (2020).
- [17] E. J. Carrell, C. M. Thorne, and G. S. Tschumper, *J. Chem. Phys.* **136**, 014103 (2012).
- [18] E. Giner, B. Pradines, A. Ferté, R. Assaraf, A. Savin, and J. Toulouse, *J. Chem. Phys.* **149**, 194301 (2018).
- [19] D. Feller, *J. Chem. Phys.* **138**, 074103 (2013).
- [20] D. S. Ranasinghe and G. A. Petersson, *J. Chem. Phys.* **138**, 144104 (2013).
- [21] D. W. Schwenke, *J. Chem. Phys.* **122**, 014107 (2005).
- [22] C. Hättig, D. P. Tew, and A. Köhn, *J. Chem. Phys.* **132**, 231102 (2010).
- [23] D. P. Tew, C. Hättig, R. A. Bachorz, and W. Klopper, in *Recent Progress in Coupled Cluster Methods – Theory and Applications*, edited by P. Čársky, J. Paldus, and J. Pittner (Springer, Dordrecht, Heidelberg, London, New York, 2010) pp. 535–572.
- [24] J. Zhang and E. F. Valeev, *J. Chem. Theory Comput.* **8**, 3175 (2012).
- [25] H.-J. Werner, T. B. Adler, G. Knizia, and F. R. Manby, in *Recent Progress in Coupled Cluster Methods – Theory and Applications*, edited by P. Čársky, J. Paldus, and J. Pittner (Springer, Dordrecht, Heidelberg, London, New York, 2010) pp. 573–620.
- [26] S. Ten-no and J. Noga, *WIREs Comput. Mol. Sci.* **2**, 114 (2012).
- [27] S. Ten-no, *Theor. Chem. Acc.* **131**, 1070 (2012).
- [28] T. Shiozaki and S. Hirata, *J. Chem. Phys.* **132**, 151101 (2010).
- [29] M. R. Nyden and G. A. Petersson, *J. Chem. Phys.* **75**, 1843 (1981).
- [30] G. A. Petersson and M. R. Nyden, *J. Chem. Phys.* **75**, 3423 (1981).
- [31] G. A. Petersson, A. Bennett, T. G. Tensfeldt, M. A. Allaham, W. A. Shirley, and J. Mantzaris, *J. Chem. Phys.* **89**, 2193 (1988).
- [32] K. D. Vogiatzis, E. C. Barnes, and W. Klopper, *Chem. Phys. Lett.* **503**, 157 (2011).
- [33] E. F. Valeev, *Phys. Chem. Chem. Phys.* **10**, 106 (2008).
- [34] A. Irmeler, A. Gallo, F. Hummel, and A. Grüneis, *Phys. Rev. Lett.* **123** (2019).
- [35] A. Irmeler and A. Grüneis, *J. Chem. Phys.* **151**, 104107 (2019).
- [36] W. Kutzelnigg and J. Morgan, *J. Chem. Phys.* **96**, 4484 (1992).
- [37] Y.-y. Ohnishi and S. Ten-no, *Mol. Phys.* **111**, 2516 (2013).
- [38] M. Schütz, G. Hetzer, and H.-J. Werner, *J. Chem. Phys.* **111**, 5691 (1999).
- [39] T. Schäfer, B. Ramberger, and G. Kresse, *J. Chem. Phys.* **146**, 104101 (2017).
- [40] M. P. Bircher, J. Villard, and U. Rothlisberger, *J. Chem. Theory Comput.* **16**, 6550 (2020).
- [41] D. Neuhauser, E. Rabani, and R. Baer, *J. Chem. Theory Comput.* **9**, 24 (2013).
- [42] A. G. Taube and R. J. Bartlett, *Collect. Czech. Chem. Commun.* **70**, 837 (2005).
- [43] J. J. Shepherd, T. M. Henderson, and G. E. Scuseria, *J. Chem. Phys.* **140**, 124102 (2014).
- [44] R. J. Bartlett and M. Musiał, *Rev. Mod. Phys.* **79**, 291 (2007).
- [45] J. Cizek and J. Paldus, *Int. J. Quantum Chem.* **5**, 359 (1971).
- [46] W. Kutzelnigg, *Theor. Chim. Acta* **68**, 445 (1985).
- [47] R. Ahlrichs, *Phys. Chem. Chem. Phys.* **8**, 3072 (2006).
- [48] T. H. Dunning, K. A. Peterson, and A. K. Wilson, *J. Chem. Phys.* **114**, 9244 (2001).
- [49] R. A. Kendall, T. H. Dunning, and R. J. Harrison, *J. Chem. Phys.* **96**, 6796 (1992).
- [50] R. M. Parrish, L. A. Burns, D. G. A. Smith, A. C. Simmonett, A. E. DePrince, E. G. Hohenstein, U. Bozkaya, A. Y. Sokolov, R. Di Remigio, R. M. Richard, J. F. Gonthier, A. M. James, H. R. McAlexander, A. Kumar, M. Saitow, X. Wang, B. P. Pritchard, P. Verma, H. F. Schaefer, K. Patkowski, R. A. King, E. F. Valeev, F. A. Evangelista, J. M. Turney, T. D. Crawford, and C. D. Sherrill, *J. Chem. Theory Comput.* **13**, 3185 (2017).
- [51] “TURBOMOLE V7.5 2020, a development of University of Karlsruhe and Forschungszentrum Karl-

- sruhe GmbH, 1989-2007, TURBOMOLE GmbH, since 2007; available from <https://www.turbomole.org>.” <https://www.turbomole.org> (2007).
- [52] S. G. Balasubramani, G. P. Chen, S. Coriani, M. Diedenhofen, M. S. Frank, Y. J. Franzke, F. Furche, R. Grotjahn, C. Harding Michael E. and Hättig, A. Hellweg, B. Helmich-Paris, C. Holzer, U. Huniar, M. Kaupp, A. Marefat Khah, S. Karbalaei Khani, T. Müller, F. Mack, B. D. Nguyen, S. M. Parker, E. Perlt, D. Rappoport, K. Reiter, S. Roy, M. Rückert, G. Schmitz, M. Sierka, E. Tapavicza, D. P. Tew, C. van Wüllen, V. K. Voora, F. Weigend, A. Wodzynski, and J. M. Yu, *J. Chem. Phys.* **152**, 184107 (2020).
- [53] R. A. Bachorz, F. A. Bischoff, A. Glöß, C. Hättig, S. Höfener, W. Klopper, and D. P. Tew, *J. Comput. Chem.* **32**, 2492 (2011).
- [54] C. Hättig, D. P. Tew, and A. Köhn, *J. Chem. Phys.* **132**, 231102 (2010).
- [55] C. Hättig, *Phys. Chem. Chem. Phys.* **7**, 59 (2005).
- [56] E. F. Valeev, “Libint: A library for the evaluation of molecular integrals of many-body operators over gaussian functions,” <http://libint.valeev.net/> (2020).
- [57] E. Solomonik, D. Matthews, J. R. Hammond, J. F. Stanton, and J. Demmel, *J. Parallel Distrib. Comput.* **74**, 3176 (2014).
- [58] M. Valiev, E. Bylaska, N. Govind, K. Kowalski, T. Straatsma, H. Van Dam, D. Wang, J. Nieplocha, E. Apra, T. Windus, and W. de Jong, *Comput. Phys. Commun.* **181**, 1477 (2010).
- [59] A. Gallo, F. Hummel, A. Irmmler, and A. Grüneis, *J. Chem. Phys.* **154**, 064106 (2021).
- [60] C. Sosa, J. Geertsen, G. W. Trucks, R. J. Bartlett, and J. A. Franz, *Chem. Phys. Lett.* **159**, 148 (1989).
- [61] W. Klopper, J. Noga, H. Koch, and T. Helgaker, *Theor. Chem. Acc.* **97**, 1432 (1997).
- [62] A. Grüneis, G. H. Booth, M. Marsman, J. Spencer, A. Alavi, and G. Kresse, *J. Chem. Theory Comput.* **7**, 2780 (2011).
- [63] K. Liao and A. Grüneis, *J. Chem. Phys.* **145**, 141102 (2016).
- [64] T. Gruber, K. Liao, T. Tsatsoulis, F. Hummel, and A. Grüneis, *Phys. Rev. X* **8**, 021043 (2018).
- [65] M. A. Morales and F. D. Malone, *J. Chem. Phys.* **153**, 194111 (2020).
- [66] A. Irmmler, A. Gallo, and A. Grüneis, (2021), 10.5281/zenodo.4597520.

Supplementary information

Appendix A: Introduction

This document presents additional data for the manuscript. Energies of the individual atoms and molecules, as well as the output of the psi4 calculations can be found in the online supplementary information in [66].

Since the geometries for all considered systems can be found in the supplementary material of Knizia *et al.* [5], we do not reiterate them here.

Appendix B: F12 results

TABLE V. BSIEs of the valence correlation energy using the (F12*) method. Calculated results use the AV{D,T,Q}Z basis sets and $\gamma \in \{1.0, 1.4\}$.

| | REc (kJ/mol) | | REo (kJ/mol) | | AEs (kJ/mol) | | IPs (kJ/mol) | | EAs (kJ/mol) | |
|----------------------|--------------|-------|--------------|-------|--------------|-------|--------------|-------|--------------|-------|
| | max | rms | max | rms | max | rms | max | rms | max | rms |
| AVDZ, $\gamma = 1.0$ | 9.859 | 3.163 | 14.625 | 4.274 | 11.957 | 5.821 | 8.375 | 4.632 | 7.059 | 4.720 |
| AVDZ, $\gamma = 1.4$ | 13.834 | 3.885 | 10.181 | 3.870 | 17.937 | 6.829 | 14.019 | 7.040 | 12.439 | 7.425 |
| AVTZ, $\gamma = 1.0$ | 3.838 | 1.434 | 5.946 | 1.657 | 3.834 | 1.520 | 2.685 | 1.393 | 1.810 | 1.189 |
| AVTZ, $\gamma = 1.4$ | 2.931 | 1.004 | 5.142 | 1.512 | 6.138 | 1.762 | 3.250 | 1.582 | 2.845 | 1.641 |
| AVQZ, $\gamma = 1.0$ | 2.233 | 0.869 | 1.727 | 0.719 | 1.795 | 0.532 | 0.898 | 0.543 | 1.015 | 0.472 |
| AVQZ, $\gamma = 1.4$ | 1.823 | 0.708 | 1.217 | 0.555 | 1.326 | 0.383 | 0.533 | 0.299 | 0.885 | 0.353 |

Appendix C: Total energies for chemical reactions

TABLE VI. Hartree-Fock (HF) energy contribution obtained with AV6Z, valence correlation energy from CCSD, and (T) contribution, both obtained from [56]-extrapolation, of the reaction energies for closed-shell systems. All energies are given in kJ/mol.

| Reaction | HF | CCSD | (T) |
|---|-----------|---------|---------|
| $\text{CO} + \text{H}_2 \rightarrow \text{HCHO}$ | 1.058 | -23.427 | 0.727 |
| $\text{CO} + \text{H}_2\text{O} \rightarrow \text{CO}_2 + \text{H}_2$ | 0.242 | -16.963 | -10.158 |
| $\text{CH}_3\text{OH} + \text{HCl} \rightarrow \text{CH}_3\text{Cl} + \text{H}_2\text{O}$ | -25.113 | -6.664 | -1.830 |
| $\text{H}_2\text{O} + \text{CO} \rightarrow \text{HCOOH}$ | -7.588 | -26.095 | -4.056 |
| $\text{CH}_3\text{OH} + \text{H}_2\text{S} \rightarrow \text{CH}_3\text{SH} + \text{H}_2\text{O}$ | -32.176 | -11.292 | -2.132 |
| $\text{CS}_2 + 2 \text{H}_2\text{O} \rightarrow \text{CO}_2 + 2 \text{H}_2\text{S}$ | -122.291 | 57.265 | 17.649 |
| $\text{HNCO} + \text{H}_2\text{O} \rightarrow \text{CO}_2 + \text{NH}_3$ | -96.839 | 9.601 | 1.302 |
| $\text{CH}_4 + \text{Cl}_2 \rightarrow \text{CH}_3\text{Cl} + \text{HCl}$ | -110.008 | 8.814 | 3.027 |
| $\text{Cl}_2 + \text{F}_2 \rightarrow 2 \text{ClF}$ | -142.439 | 22.963 | 6.220 |
| $\text{CO} + \text{Cl}_2 \rightarrow \text{COCl}_2$ | -56.532 | -48.165 | -10.090 |
| $\text{CO}_2 + 3 \text{H}_2 \rightarrow \text{CH}_3\text{OH} + \text{H}_2\text{O}$ | -118.688 | -14.650 | 15.493 |
| $\text{HCHO} + \text{H}_2 \rightarrow \text{CH}_3\text{OH}$ | -119.505 | -8.186 | 4.608 |
| $\text{CO} + 2 \text{H}_2 \rightarrow \text{CH}_3\text{OH}$ | -118.447 | -31.614 | 5.335 |
| $\text{SO}_3 + \text{CO} \rightarrow \text{SO}_2 + \text{CO}_2$ | -159.381 | -15.010 | -6.383 |
| $\text{H}_2 + \text{Cl}_2 \rightarrow 2 \text{HCl}$ | -213.351 | 15.976 | 6.784 |
| $\text{C}_2\text{H}_2 + \text{H}_2 \rightarrow \text{C}_2\text{H}_4$ | -216.388 | 5.679 | 4.369 |
| $\text{SO}_2 + \text{H}_2\text{O}_2 \rightarrow \text{SO}_3 + \text{H}_2\text{O}$ | -231.750 | 16.268 | 4.335 |
| $\text{CO} + 3 \text{H}_2 \rightarrow \text{CH}_4 + \text{H}_2\text{O}$ | -246.902 | -31.115 | 7.262 |
| $\text{HCN} + 3 \text{H}_2 \rightarrow \text{CH}_4 + \text{NH}_3$ | -335.389 | 3.306 | 11.059 |
| $\text{H}_2\text{O}_2 + \text{H}_2 \rightarrow 2 \text{H}_2\text{O}$ | -391.373 | 18.221 | 8.110 |
| $\text{CO} + \text{H}_2\text{O}_2 \rightarrow \text{CO}_2 + \text{H}_2\text{O}$ | -391.131 | 1.258 | -2.048 |
| $2 \text{NH}_3 + 3 \text{Cl}_2 \rightarrow \text{N}_2 + 6 \text{HCl}$ | -482.764 | 63.682 | 11.655 |
| $3 \text{N}_2\text{H}_4 \rightarrow 4 \text{NH}_3 + \text{N}_2$ | -470.681 | 32.160 | -0.570 |
| $\text{H}_2 + \text{F}_2 \rightarrow 2 \text{HF}$ | -610.736 | 32.890 | 12.878 |
| $\text{CH}_4 + 4 \text{H}_2\text{O}_2 \rightarrow \text{CO}_2 + 6 \text{H}_2\text{O}$ | -1318.348 | 87.035 | 15.020 |
| $2 \text{NH}_3 + 3 \text{F}_2 \rightarrow \text{N}_2 + 6 \text{HF}$ | -1674.919 | 114.422 | 29.936 |

TABLE VII. Open-shell systems (REo). The interpretation of the columns is as in Table VI.

| Reaction | HF | CCSD | (T) |
|--|-----------|----------|---------|
| HCl + H → Cl + H ₂ | -28.206 | 12.237 | 6.653 |
| H ₂ O + F ₂ → 2 HF + O | -310.135 | 232.071 | 27.904 |
| OH + H ₂ → H ₂ O + H | -14.235 | -45.143 | -7.958 |
| CO + OH → CO ₂ + H | -13.994 | -62.106 | -18.116 |
| S + 2 HCl → H ₂ S + Cl ₂ | 21.046 | -123.055 | -16.659 |
| N + O ₂ → NO + O | -110.043 | -30.128 | 0.832 |
| 4 HCl + O ₂ → 2 H ₂ O + Cl ₂ | -63.503 | -86.576 | -4.193 |
| 2 NO → N ₂ + O ₂ | -141.430 | -30.529 | -3.550 |
| 2 H ₂ O ₂ → 2 H ₂ O + O ₂ | -292.541 | 91.065 | 6.845 |
| Cl ₂ + H → HCl + Cl | -241.557 | 28.214 | 13.437 |
| 2 SO ₂ + O ₂ → 2 SO ₃ | -170.959 | -58.530 | 1.825 |
| Cl + OH → HOCl | -43.344 | -180.661 | -21.899 |
| H ₂ S + F ₂ → S + 2 HF | -418.431 | 139.968 | 22.753 |
| 2 NH ₂ → N ₂ H ₄ | -136.148 | -153.938 | -14.755 |
| NO + N → O + N ₂ | -251.473 | -60.657 | -2.717 |
| O + 2 HCl → H ₂ O + Cl ₂ | -87.251 | -215.157 | -21.810 |
| SO ₂ + O → SO ₃ | -140.979 | -201.134 | -18.801 |
| CS + O → CO + S | -319.067 | -54.285 | 6.553 |
| CH ₃ OH + O → HCHO + H ₂ O | -181.096 | -190.995 | -19.633 |
| NH + H → NH ₂ | -277.962 | -131.485 | -5.679 |
| Si + 2 H ₂ → SiH ₄ | -373.824 | -64.824 | -3.810 |
| CS + S → CS ₂ | -280.543 | -143.489 | -25.977 |
| NH ₂ + H → NH ₃ | -348.191 | -127.825 | -6.023 |
| 2 H ₂ + O ₂ → 2H ₂ O | -490.204 | -54.624 | 9.376 |
| CO ₂ + C → 2 CO | -425.583 | -104.610 | -9.449 |
| C + H ₂ O → CO + H ₂ | -425.342 | -121.574 | -19.607 |
| N ₂ H ₄ + O ₂ → N ₂ + 2 H ₂ O | -542.239 | -33.402 | 3.387 |
| 2 NH + NH → N ₂ + H ₂ | -393.195 | -288.506 | -32.102 |
| C + S ₂ → CS ₂ | -472.107 | -224.499 | -36.431 |
| 2 CO + 2 NO → N ₂ + 2 CO ₂ | -631.152 | -119.080 | -14.490 |
| CH ₄ + 2 O ₂ → CO ₂ + 2 H ₂ O | -733.265 | -95.096 | 1.331 |
| 4 NH ₃ + 5 O ₂ → 4 NO + 6 H ₂ O | -873.176 | -71.306 | 17.830 |
| 2 NH ₃ + 2 NO + O → 2 N ₂ + 3 H ₂ O | -774.948 | -268.581 | -17.898 |
| C + O ₂ → CO ₂ | -915.304 | -193.161 | -20.390 |
| CS ₂ + 3 O ₂ → CO ₂ + 2 SO ₂ | -900.329 | -224.948 | -13.949 |
| CH ₄ + 4 NO → 2 N ₂ + CO ₂ + 2 H ₂ O | -1016.126 | -156.154 | -5.768 |
| CH ₄ + NH ₃ + 3 O → HCN + 3 H ₂ O | -566.415 | -600.848 | -56.136 |
| 2 C + H ₂ → C ₂ H ₂ | -875.468 | -315.782 | -35.796 |
| 4 NH ₃ + 3 O ₂ → 2 N ₂ + 6 H ₂ O | -1156.037 | -132.365 | 10.730 |

TABLE VIII. Atomization energies (AEs). The interpretation of the columns is as in Table VI.

| Reaction | HF | CCSD | (T) |
|--|----------|---------|--------|
| F ₂ | -151.770 | 281.165 | 31.299 |
| Cl ₂ | 81.149 | 147.632 | 20.090 |
| ClF | 35.909 | 202.917 | 22.585 |
| ClO | 25.919 | 217.176 | 26.213 |
| NH | 215.115 | 126.599 | 4.605 |
| CH | 238.401 | 108.830 | 3.647 |
| S ₂ | 215.312 | 185.460 | 30.731 |
| OH | 286.366 | 154.038 | 7.068 |
| HCl | 322.705 | 119.418 | 6.653 |
| P ₂ | 155.695 | 286.663 | 41.507 |
| O ₂ | 110.998 | 343.738 | 39.427 |
| SO | 226.121 | 263.028 | 33.588 |
| SiH ₂ (³ B ₁) | 446.960 | 108.617 | 1.951 |
| HF | 404.939 | 177.728 | 9.210 |
| NO | 221.041 | 373.866 | 38.595 |
| SiH ₂ (¹ A ₁) | 463.613 | 176.108 | 3.550 |
| PH ₂ | 456.840 | 182.551 | 4.918 |
| HOCl | 329.710 | 334.699 | 28.967 |
| CS | 406.876 | 266.470 | 41.186 |
| CN | 372.902 | 326.804 | 42.278 |
| CH ₂ (¹ A ₁) | 531.275 | 216.344 | 8.168 |
| NH ₂ | 493.077 | 258.084 | 10.284 |
| SH ₂ | 543.216 | 214.259 | 9.875 |
| CH ₂ (³ B ₁) | 649.215 | 141.029 | 4.072 |
| SiO | 459.809 | 304.986 | 36.431 |
| N ₂ | 472.514 | 434.523 | 41.312 |
| H ₂ O | 651.513 | 306.362 | 15.026 |
| PH ₃ | 723.682 | 278.878 | 8.265 |
| CO | 725.943 | 320.755 | 34.633 |
| SO ₂ | 447.220 | 564.611 | 69.788 |
| H ₂ O ₂ | 560.741 | 523.764 | 38.162 |
| HCO | 762.065 | 365.317 | 34.985 |
| NH ₃ | 841.268 | 385.909 | 16.307 |
| HCN | 827.211 | 434.722 | 39.711 |
| SiH ₄ | 1075.646 | 279.185 | 3.810 |
| H ₂ CO | 1075.799 | 451.360 | 33.906 |
| CO ₂ | 1026.303 | 536.899 | 59.817 |
| CH ₃ Cl | 1242.518 | 386.450 | 22.755 |
| C ₂ H ₂ | 1226.379 | 422.963 | 35.796 |
| CH ₄ | 1374.066 | 367.050 | 12.345 |
| N ₂ H ₄ | 1122.301 | 670.106 | 35.323 |
| CH ₃ SH | 1470.091 | 485.920 | 26.279 |
| CH ₃ OH | 1546.212 | 566.730 | 29.298 |
| C ₂ H ₄ | 1793.679 | 524.465 | 31.427 |

TABLE IX. Ionization potentials (IPs). The interpretation of the columns is as in Table VI.

| Reaction | HF | CCSD | (T) |
|---|----------|---------|---------|
| Si | 736.815 | 44.959 | 4.710 |
| B | 776.056 | 15.921 | 4.035 |
| PH ₂ (¹ A ₁) | 899.494 | 42.593 | 5.107 |
| PH | 931.346 | 45.356 | 5.117 |
| S | 891.226 | 100.008 | 4.794 |
| SH | 885.263 | 111.476 | 6.797 |
| SH ₂ (² B ₁) | 888.222 | 114.845 | 8.155 |
| P | 955.635 | 53.867 | 5.595 |
| C | 1042.056 | 38.083 | 3.153 |
| Cl ₂ | 1045.498 | 70.474 | -1.767 |
| O ₂ | 1205.821 | -25.801 | -9.885 |
| H ₂ O | 1054.632 | 158.840 | 10.092 |
| ClF | 1126.613 | 96.558 | 1.980 |
| HCl | 1110.361 | 117.113 | 7.824 |
| Cl | 1134.933 | 110.247 | 6.075 |
| OH | 1094.944 | 155.435 | 7.858 |
| O | 1160.072 | 146.196 | 5.335 |
| CO | 1256.449 | 97.480 | 2.174 |
| N | 1340.575 | 57.603 | 3.004 |
| N ₂ (² S _g) | 1519.395 | 2.990 | -14.438 |
| HF | 1373.084 | 173.280 | 9.399 |
| F | 1510.014 | 164.236 | 6.611 |

TABLE X. Electron affinities (EAs). The interpretation of the columns is as in Table VI.

| Reaction | HF | CCSD | (T) |
|-----------------|----------|----------|---------|
| P | 31.078 | -94.038 | -7.435 |
| NH ₂ | 103.844 | -158.824 | -17.433 |
| PH | 16.546 | -104.266 | -9.326 |
| PO | -75.123 | -32.123 | -0.226 |
| CH | -40.900 | -65.231 | -8.102 |
| C | -43.505 | -69.363 | -7.682 |
| SiH | -72.351 | -42.481 | -6.312 |
| PH ₂ | -4.070 | -106.120 | -10.365 |
| Si | -81.724 | -48.047 | -6.800 |
| O | 55.461 | -179.319 | -16.165 |
| S ₂ | -78.114 | -79.944 | -3.429 |
| OH | 25.985 | -183.877 | -19.137 |
| S | -85.119 | -106.677 | -9.307 |
| SH | -102.303 | -112.532 | -11.051 |
| F | -113.293 | -199.609 | -17.460 |
| CN | -278.623 | -101.386 | -1.919 |

Appendix D: Further correlation energy statistics

TABLE XI. BSIEs of the Hartree–Fock energies with the reference obtained from AV6Z. BSIEs of conventional CCSD valence correlation energy with the reference obtained from [56]-extrapolation.

| | REc (kJ/mol) | | REo (kJ/mol) | | AEs (kJ/mol) | | IPs (kJ/mol) | | EAs (kJ/mol) | |
|-------------|--------------|--------|--------------|--------|--------------|--------|--------------|--------|--------------|--------|
| | max | rms | max | rms | max | rms | max | rms | max | rms |
| HF @ AVTZ | 6.519 | 2.523 | 15.598 | 3.563 | 10.489 | 3.023 | 2.964 | 1.258 | 2.040 | 0.833 |
| HF @ AVQZ | 1.898 | 0.691 | 6.619 | 1.287 | 3.689 | 0.726 | 0.859 | 0.282 | 0.593 | 0.259 |
| HF @ AV5Z | 0.625 | 0.187 | 2.145 | 0.412 | 1.226 | 0.238 | 0.200 | 0.076 | 0.131 | 0.069 |
| CCSD @ AVDZ | 44.190 | 14.396 | 75.092 | 34.859 | 118.182 | 56.849 | 44.421 | 29.628 | 29.792 | 20.463 |
| CCSD @ AVTZ | 19.844 | 6.744 | 41.541 | 17.175 | 41.097 | 21.667 | 18.297 | 11.426 | 12.558 | 7.862 |
| CCSD @ AVQZ | 9.974 | 2.731 | 17.478 | 6.550 | 16.732 | 8.263 | 7.527 | 4.503 | 4.295 | 2.889 |
| CCSD @ AV5Z | 5.668 | 1.476 | 8.772 | 3.170 | 8.165 | 4.045 | 3.880 | 2.279 | 2.258 | 1.465 |
| CCSD @ AV6Z | 3.269 | 0.852 | 5.075 | 1.833 | 4.721 | 2.340 | 2.245 | 1.319 | 1.305 | 0.848 |

TABLE XII. BSIE of the valence correlation energy of CCSD(T) for the different reactions. Reference energy is obtained from [56]-extrapolation. FPa energies as described in main text together with (T*) using 12 FNOs per occupied and [34]-extrapolation from MP2 for the correction. FPb energies include (T*) correction using 20 FNOs per occupied and an MP2 estimate obtained from [45]-extrapolation.

| Method | REc (kJ/mol) | | REo (kJ/mol) | | AEs (kJ/mol) | | IPs (kJ/mol) | | EAs (kJ/mol) | |
|------------------------------|--------------|-------|--------------|--------|--------------|-------|--------------|-------|--------------|-------|
| | max | rms | max | rms | max | rms | max | rms | max | rms |
| [23] | 14.007 | 6.077 | 33.924 | 10.270 | 25.533 | 8.229 | 9.000 | 4.317 | 5.766 | 2.993 |
| [34] | 7.173 | 2.254 | 4.839 | 2.080 | 4.196 | 1.940 | 1.914 | 0.796 | 1.716 | 0.894 |
| [45] | 1.255 | 0.465 | 1.998 | 0.713 | 1.397 | 0.609 | 0.252 | 0.127 | 0.242 | 0.143 |
| FPa + Δ ps-ppl + (T*) | 7.714 | 2.639 | 9.877 | 3.423 | 11.401 | 2.944 | 3.754 | 1.861 | 7.473 | 2.260 |
| FPb + Δ ps-ppl + (T*) | 3.565 | 1.144 | 2.333 | 1.030 | 4.255 | 0.908 | 1.874 | 0.844 | 4.179 | 1.115 |

TABLE XIII. BSIE of the CCSD(T) energy for the different reactions. For the reference the Hartree–Fock energy is obtained using the AV6Z basis set. The CCSD(T) valence correlation part is obtained from [56]-extrapolation. Focal-point correlation energies as described in Table XII with Hartree–Fock energies obtained from AVQZ and AV5Z for FPa and FPb, respectively.

| Method | REc (kJ/mol) | | REo (kJ/mol) | | AEs (kJ/mol) | | IPs (kJ/mol) | | EAs (kJ/mol) | |
|------------------------------|--------------|-------|--------------|--------|--------------|--------|--------------|-------|--------------|-------|
| | max | rms | max | rms | max | rms | max | rms | max | rms |
| [23] | 20.195 | 8.360 | 49.522 | 13.512 | 36.022 | 10.933 | 7.863 | 3.423 | 4.994 | 2.472 |
| [34] | 8.097 | 2.635 | 6.065 | 2.478 | 3.781 | 1.756 | 2.426 | 1.028 | 2.106 | 1.072 |
| [45] | 1.510 | 0.526 | 2.027 | 0.762 | 1.271 | 0.489 | 0.331 | 0.178 | 0.315 | 0.175 |
| FPa + Δ ps-ppl + (T*) | 8.638 | 3.037 | 16.496 | 4.352 | 11.727 | 3.421 | 3.660 | 1.674 | 7.641 | 2.238 |
| FPb + Δ ps-ppl + (T*) | 3.819 | 1.195 | 3.198 | 1.248 | 4.316 | 0.927 | 1.882 | 0.819 | 4.185 | 1.115 |